inant kinetic pathway for the coordinating general acids.

Conclusions

Acids can accelerate the ring opening of polyamine chelate complexes of nickel(II) by direct protonation of the nitrogen donor while the donor is still within the first coordination sphere. Acid attack at the amine nitrogen occurs prior to or during solvent replacement of the donor. The relative importance of the protonation and the solvent-separation pathways is controlled by those factors which prevent the donor atom from moving smoothly out of the first coordination sphere. The effect of the chelate ring is greater than that of a solvent cage.

Although the effect of coordinating general acids has been observed in other situations, it is unique that the effect occurs for a series of uncharged carboxylic acids. It is also important that these acids can, at high concentration, assist the ring opening of nickel(II) polyamine complexes.

Acknowledgment. This investigation was supported by Public Health Service Grant No. GM-12152 from the National Institute of General Medical Sciences.

Registry No. $Ni(en)^{2+}(aq)$, 15615-30-2; $Ni(en)_3^{2+}$, 15390-99-5; $NiNH_3^{2+}(aq)$, 18042-21-2; CH_3COOH, 64-19-7; $ClCH_2COOH$, 79-11-8; $Cl_2CHCOOH$, 79-43-6; Cl_3CCOOH, 76-03-9; $C_5H_5NH^+$, 16969-45-2.

Contribution from the Department of Chemistry, Purdue University, West Lafayette, Indiana 47907

Kinetics of the Acid-Catalyzed Dissociation of Nickel(II) Triglycine

CHARLES E. BANNISTER and DALE W. MARGERUM*

Received December 8, 1980

As the concentration of acid increases, more than one proton assists the rate of dissociation of the doubly deprotonated triglycine nickel(II) complex, $Ni(H_{-2}G_3)^-$. The observed first-order rate constant equals $k_{H_2O} + k_H[H^+] + k_{H,H}[H^+]^2 + (k_{HB} + k_{H,HB}[H^+])[HB]$, where HB is a general acid. The k_{HB} and $k_{H,HB}$ rate constants increase with the acid strength of HB, but the Brønsted α value decreases as the acid strength increases. The values for the H_3O^+ rate constants are $k_H = 9.5 \times 10^4\ M^{-1}\ s^{-1}$ and $k_{H,H} = 1.1 \times 10^8\ M^{-2}\ s^{-1}$. A modified Marcus theory of proton transfer is used to fit the Brønsted plot for the single-proton pathway. A large W_R term is required, and this is attributed to the need to solvate the nickel ion in the reaction complex. Mixed complexes in which ligands block axial coordination by solvent are not general-acid catalyzed.

Introduction

Triglycine (glycylglycylglycine, G_3) forms a yellow, square-planar complex (structure I) with nickel(II) in which

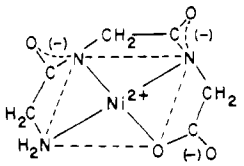

I

coordination of the peptide nitrogens results in ionization of the two peptide hydrogens.[1-3] Previous kinetic studies with the $Ni(H_{-2}G_3)^-$ complex showed that proton transfer to the peptide nitrogen is subject to general-acid catalysis.[3-6] The resulting Brønsted plots for the reaction in Scheme I are unusual. Although they resemble the behavior of Eigen's plots[7] for normal acids and bases and include a transition of the α value from 1 to 0, they differ from Eigen's plots in that the H_3O^+ rate constant is many orders of magnitude below the diffusion-controlled limit.

In the present work, we extend the study of general-acid catalysis with $Ni(H_{-2}G_3)^-$ to include a series of acids with pK_a values between those of acetic acid ($pK_a = 4.64$) and H_3O^+ ($pK_a = -1.74$) (Figure 1). The present studies had to be carried out in higher concentrations of acid than used before, and two additional terms were found for the rate of acid decomposition of $Ni(H_{-2}G_3)^-$. One term exhibited a $[H^+]^2$ dependence and the other a $[H^+][HB]$ dependence. The behavior of the Brønsted plot with general acids can be accounted for by use of a modified[8,9] Marcus theory,[10,11] in which the intrinsic proton barrier ($\lambda/4$) is small, but a substantial input of work (W_R) is needed in order to form the reaction complex prior to proton transfer. The reaction complex differs from an encounter complex in that the W_R term is much larger. This work appears to be associated with the need to solvate the nickel(II). The behavior of coordinating ligands such as α-picoline, which block axial solvation of the nickel, support this explanation.

Scheme I. Direct Protonation of the Peptide Nitrogen

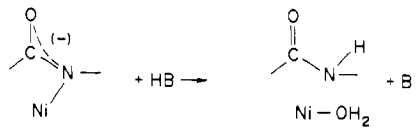

Experimental Section

Nickel(II) perchlorate was prepared from nickel(II) carbonate and perchloric acid. Stock solutions were standardized by EDTA titration using murexide indicator. Nickel(II) triglycine solutions ($(2-4) \times 10^{-3}$ M) were prepared just prior to each set of experiments. The chromatographically pure triglycine (Sigma Chemical) was added in a 2:1 mole ratio to a nickel(II) perchlorate solution. The bright yellow $Ni(H_{-2}G_3)^-$ complex formed as the pH of the solution was

(1) Kim, M. K.; Martell, A. E. *J. Am. Chem. Soc.* **1967**, *89*, 5138.
(2) Martin, R. B.; Chamberlin, M.; Edsall, J. T. *J. Am. Chem. Soc.* **1960**, *82*, 495.
(3) Billo, E. J.; Margerum, D. W. *J. Am. Chem. Soc.* **1970**, *92*, 6811.
(4) Paniago, E. B.; Margerum, D. W. *J. Am. Chem. Soc.* **1972**, *94*, 6704.
(5) Bannister, C. E.; Margerum, D. W.; Raycheba, J. M. T.; Wong, L. F. *Symp. Faraday Soc.* **1975**, *No. 10*, 78.
(6) Pagenkopf, G. K.; Margerum, D. W. *J. Am. Chem. Soc.* **1968**, *90*, 6963.
(7) Eigen, M. *Angew. Chem., Int. Ed. Engl.* **1964**, *3*, 1.
(8) Kreevoy, M. M.; Konasewich, D. E. *Adv. Chem. Phys.* **1972**, *21*, 243.
(9) Hassid, A. I.; Kreevoy, M. M.; Liang, T.-M. *Symp. Faraday Soc.* **1975**, *No. 10*, 69.
(10) Cohen, A. O.; Marcus, R. A. *J. Phys. Chem.* **1968**, *72*, 4249.
(11) Marcus, R. A. *J. Phys. Chem.* **1968**, *72*, 891.

0020-1669/81/1320-3149$01.25/0

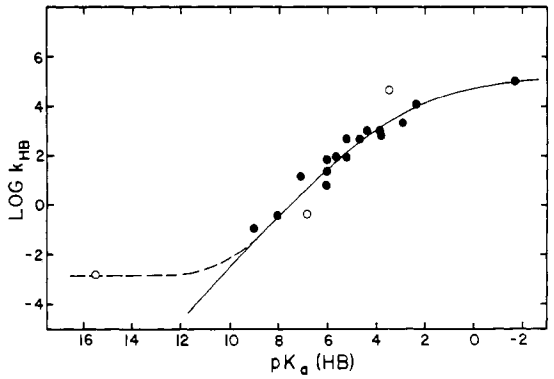

Figure 1. Brønsted plot for the acid-dissociation reaction of Ni($H_{-2}G_3$)$^-$. From left to right the solid circles refer to the general acids, HB: H_3BO_3, H(Tris)$^+$, H(Im)$^+$, H_2EDTA^{2-}, H(α-pic)$^+$, H(β-pic)$^+$, H(mal)$^-$, H(py)$^+$, H(suc)$^-$, acetic acid, H(fum)$^-$, glycolic acid, formic acid, chloroacetic acid, H_2(gly)$^+$, and H_3O^+. The solid line was calculated with use of eq 19–21 with W_R = 10.5 kcal mol^{-1}, $\lambda/4$ = 1.6 kcal mol^{-1}, C = 3.5 kcal mol^{-1}, and $k_{HB} = (\bar{k}T/h)\exp(-\Delta G^*/RT)$. The open circles refer to H_2O, H(PIPES)$^-$, and H(ox)$^-$; see text.

slowly adjusted to 9.5–10 with NaOH. The ionic strength was adjusted to 0.30 M $NaClO_4$.

Pyridine, α-picoline, and β-picoline were all vacuum distilled twice. Tris(hydroxymethyl)aminomethane (Tris) was recrystallized from a hot water–methanol solution and dried in vacuo. $NaClO_4$ solutions were prepared by neutralization of Na_2CO_3 with perchloric acid. Other stock solutions were either standardized by acid–base titration or prepared from the dried reagent grade chemicals.

Kinetic Measurements. The rate of disappearance of Ni($H_{-2}G_3$)$^-$ was followed spectrophotometrically at 430 nm (ϵ = 260 M^{-1} cm^{-1}) with use of a Durrum stopped-flow spectrophotometer interfaced to a Hewlett-Packard 2115A digital computer[12] and thermostated at 25 ± 0.1 °C. With excess buffer and constant pH, excellent first-order reactions were observed. After each run, linear and nonlinear regression analysis (over at least 4 half-lives) gave k_{obsd}, the initial absorbance (A_0), and the final absorbance (A_∞) (eq 1). All reported first-order rate constants are the average of at least three replicates.

$$A - A_\infty = (A_0 - A_\infty)e^{-k_{obsd}t} \qquad (1)$$

pH Measurements. All pH measurements were thermostated at 25.0 ± 0.1 °C. The relationship between −log [H$^+$] and pH was determined by titration of $HClO_4$ with NaOH using Sargent-Welch electrodes (saturated NaCl reference) and is given by −log[H$^+$] = pH + 0.10 when the ionic strength is 0.30 M $NaClO_4$.

Equilibrium Measurements. The stability constant for the α-picoline adduct [Ni($H_{-2}G_3$)(α-pic)]$^-$ was determined at 430 nm with use of a Cary 14 spectrophotometer. Because a slow displacement reaction follows the initial adduct formation, the stability constant for the imidazole adduct [Ni($H_{-2}G_3$)Im]$^-$ was determined from the initial absorbance jump observed at 430 nm with a Durrum stopped-flow spectrophotometer. The stability constants were determined at 25.0 ± 0.1 °C and 0.30 M $NaClO_4$ with the relationship given by eq 2, where ϵ (absorbance divided by the product of the path length and [Ni($H_{-2}G_3$)$^-$]$_T$) is related to the absorptivities of Ni($H_{-2}G_3$)$^-$ (ϵ_{NiL}) and [Ni($H_{-2}G_3$)B]$^-$ (ϵ_{NiLB}) by the stability constant (K_B).

$$\epsilon = \frac{\epsilon_{NiL} - \epsilon}{K_B[B]} + \epsilon_{NiLB} \qquad (2)$$

Results and Discussion

The overall reaction for the acid decomposition of Ni($H_{-2}G_3$)$^-$ (eq 3) was studied kinetically under irreversible

$$Ni(H_{-2}G_3)^- + 3H^+ \rightarrow Ni^{2+}(aq) + HG_3^{\pm} \qquad (3)$$

conditions (pH 6.6–2.9) in the presence of several weak acids. The rate of disappearance of the square-planar complex (λ_{max} = 430 nm) at constant pH followed the first-order rate expression (eq 4), where k_{obsd} was experimentally determined as a function of both the pH ([HB] + [B] constant) and the general-acid concentration (constant pH).

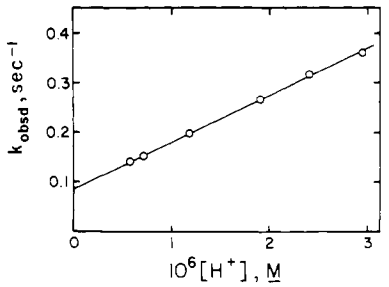

Figure 2. Plot of the dependence of k_{obsd} on the concentration of H_3O^+ showing the first-order dependence at pH >5 (0.30 M $NaClO_4$).

$$-\frac{d[Ni(H_{-2}G_3)^-]_T}{dt} = k_{obsd}[Ni(H_{-2}G_3)^-]_T \qquad (4)$$

Previous kinetics studies[3] of the protonation of Ni($H_{-2}G_3$)$^-$ (pH >4) indicated that the reaction was general-acid catalyzed and that the first-order rate constant was given by eq 5. The

$$k_{obsd} = k_{H_2O} + k_H[H^+] + k_{HB}[HB] \qquad (5)$$

proposed mechanism, consistent with this rate law, is given by eq 6 and 7. Because of the difference in the electronic state

$$Ni(H_{-2}G_3)^- + HB \xrightarrow{k_{HB}} Ni(H_{-1}G_3) + B \qquad (6)$$

$$Ni(H_{-1}G_3) + 2H^+ \xrightarrow{fast} Ni(aq)^{2+} + HG_3^{\pm} \qquad (7)$$

and coordination between the square-planar Ni($H_{-2}G_3$)$^-$ complex and the octahedral Ni($H_{-1}G_3$) complex,[3] the first proton transfer to the peptide nitrogen (eq 6) is rate limiting.

The first-order dependence of k_{obsd} on [HB] (eq 5) is further verified for several other acids (Table I) at −log [H$^+$] > 4. For the acids given in Table II, the resolved rate constants (k_{HB}) were obtained with use of eq 5. With each acid, the concentration of [HB]$_T$ present as HB was determined with use of the acid dissociation constant (K_a) for HB. With the acids H_2EDTA^{2-}, H(py)$^+$, and H(Tris)$^+$, an additional pathway (eq 8 and 9) for the reaction of the conjugate base with Ni($H_{-2}G_3$)$^-$

$$Ni(H_{-2}G_3)^- + B \xrightarrow{k_B} [Ni(H_{-2}G_3)B]^- \qquad (8)$$

$$[Ni(H_{-2}G_3)B] + 3H^+ \xrightarrow{fast} Ni(aq)^{2+} + B + HG_3^{\pm} \qquad (9)$$

was also observed. This pathway has been observed for several other bases and involves a nucleophilic reaction of the base with Ni($H_{-2}G_3$)$^-$ followed by rapid peptide protonation.[13]

H,HB Pathway. Another reaction pathway, not previously observed, is detected when the protonation of Ni($H_{-2}G_3$)$^-$ is studied at pH <4 (Table III). As shown by Figure 2, the rate for Ni($H_{-2}G_3$)$^-$ protonation has a first-order dependence on the H_3O^+ concentrations at high pH values. This is consistent with the previously reported behavior (eq 5).[3] However, a [H$^+$]^2 dependence and a [H$^+$][HB] dependence is observed at pH <4 (Figure 3). Upon the addition of acid, there is no initial absorbance change at 430 nm prior to the observed reaction, suggesting that the Ni($H_{-2}G_3$)$^-$ remains the dominant reactant in solution.

The kinetic behavior observed for Ni($H_{-2}G_3$)$^-$ dissociation at pH <4 is consistent with a pathway (eq 10 and 11) in which

$$Ni(H_{-2}G_3)^- + H^+ \rightleftharpoons Ni(H_{-2}G_3)H \qquad (10)$$

$$Ni(H_{-2}G_3)H + HB \xrightarrow{k_{HB}^H} Ni(aq)^{2+} + G_3^- \qquad (11)$$

(12) Willis, B. G.; Bittikoffer, J. A.; Pardue, H. L.; Margerum, D. W. *Anal. Chem.* **1970**, *42*, 1340.

(13) Billo, E. J.; Smith, G. F.; Margerum, D. W. *J. Am. Chem. Soc.* **1971**, *93*, 2635.

Table I. Observed Rate Constants for the Protonation of $Ni(H_{-2}G_3)^-$ by HB (25.0 °C, 0.30 M $NaClO_4$)[a]

HB	$[HB]_T$, M	−log $[H^+]$	k_{obsd}, s^{-1}
$H_2(gly)^+$ [b]	0.050	6.23	0.426 ± 0.001
	0.10	6.20	0.494 ± 0.001
	0.20	6.18	0.642 ± 0.001
	0.30	6.17	0.809 ± 0.002
$H(ox)^-$ [c]	0.010	6.18	1.20 ± 0.01
	0.020	6.20	2.18 ± 0.03
	0.030	6.18	3.25 ± 0.02
$H(fum)^-$ [d]	0.020	4.60	55 ± 1
	0.020	4.21	92 ± 2
	0.040	4.57	63 ± 1
	0.040	4.20	105 ± 1
	0.060	4.55	69 ± 1
	0.060	4.18	117 ± 2
$H(suc)^-$ [c]	0.0050	6.18	0.566 ± 0.001
	0.010	6.19	0.835 ± 0.001
	0.015	6.17	1.19 ± 0.01
$H(py)^+$	0.050	5.37	2.71 ± 0.01
	0.050	5.19	3.22 ± 0.01
	0.10	5.61	3.49 ± 0.01
	0.10	5.34	4.87 ± 0.01
	0.10	5.16	5.77 ± 0.01
	0.10	4.90	6.99 ± 0.02
	0.15	5.63	5.02 ± 0.01
	0.15	5.34	7.03 ± 0.02
	0.15	5.16	8.04 ± 0.02
	0.15	4.89	9.69 ± 0.02
	0.20	4.89	12.2 ± 0.1
	0.24	5.66	7.61 ± 0.02
	0.28	5.67	8.79 ± 0.01
	0.30	5.68	9.22 ± 0.02
	0.40	5.67	12.0 ± 0.1
$H_2(EDTA)^{2-}$ [e]	0	6.15	0.151 ± 0.001
	0.0060	6.11	0.214 ± 0.001
	0.010	6.12	0.253 ± 0.001
	0.014	6.11	0.301 ± 0.001
	0.015	6.72	0.164 ± 0.001
	0.015	6.24	0.271 ± 0.001
	0.017	6.72	0.177 ± 0.001
	0.017	6.24	0.289 ± 0.001
	0.020	6.72	0.195 ± 0.001
	0.020	6.23	0.326 ± 0.002
	0.020	6.11	0.369 ± 0.001
	0.030	6.71	0.254 ± 0.001
	0.030	6.21	0.426 ± 0.001
$H(\beta\text{-pic})^+$ [e]	0.040	6.52	0.684 ± 0.007
	0.080	6.54	1.27 ± 0.02
	0.10	6.55	1.58 ± 0.02
	0.14	6.56	2.18 ± 0.01
	0.18	6.58	2.68 ± 0.02
	0.24	6.60	3.40 ± 0.01
	0.30	6.63	4.00 ± 0.03
$H(MES)^+$	0.036	5.31	0.526 ± 0.002
	0.090	5.34	0.523 ± 0.002
	0.21	5.29	0.530 ± 0.002
	0.30	5.30	0.526 ± 0.002
$H(PIPES)^-$ [e]	0	6.15	0.146 ± 0.001
	0.050	6.13	0.163 ± 0.001
	0.050	5.92	0.208 ± 0.001
	0.070	5.91	0.217 ± 0.001
	0.080	6.14	0.174 ± 0.002
	0.090	5.90	0.229 ± 0.001
$H(Tris)^+$ [e]	0	6.45	0.109 ± 0.002
	0.050	6.44	0.141 ± 0.001
	0.050	6.15	0.176 ± 0.002
	0.050	5.95	0.208 ± 0.001
	0.070	6.44	0.155 ± 0.002
	0.080	6.15	0.191 ± 0.001
	0.080	5.96	0.222 ± 0.002
	0.090	6.46	0.166 ± 0.002
	0.11	6.17	0.200 ± 0.001
	0.11	5.97	0.234 ± 0.001

[a] $[Ni(H_{-2}G_3)]_T = 1.0 \times 10^{-3}$ M, 403 nm. Abbreviations: gly, glycate; ox, oxalate; fum, fumarate; suc, succinate; py, pyridine. [b] 0.020 M $[MES]_T$. [c] 0.036 M $[MES]_T$, 0.0160 M $[EDTA]_T$. [d] 0.10 M $[HOAc]_T$. [e] 0.10 M $[MES]_T$.

Table II. General-Acid Rate Constants for the Reaction of HB with $Ni(H_{-2}G_3)^-$ (0.30 M $NaClO_4$, 25.0 °C)

HB	pK_a(HB)	k_{HB}, M^{-1} s^{-1}	k_B, M^{-1} s^{-1}
$H_2(gly)^+$	2.33[a]	1.1×10^4	
$H(ox)^-$	3.51[b]	4.9×10^4	
$H(fum)^-$	4.39[c]	9.5×10^3	
$H(suc)^-$	5.28[d]	5.7×10^3	
$H(py)^+$	5.33[e]	6.6×10	1.7×10
$H(mal)^-$ [f]	5.70[f]	1.0×10^3	
H_2EDTA^{2-}	6.00[g]	2.2×10	3.2
$H(\beta\text{-pic})^+$	6.00[e]	7.0×10	
$H(MES)^+$	6.2[h]	5.0×10^{-1}	
$H(PIPES)^-$	6.8[h]	5.0×10^{-1}	
$H(Tris)^+$	8.07[i]	3.3×10^{-1}	1.4×10
boric acid[f]	9.0[f]	1.0×10^{-1}	
H_2O	15.52	8.6×10^{-2}	

[a] Sigel, H.; Griesser, R. *Helv. Chim. Acta* 1967, *50*, 1842. [b] McAuley, A.; Nancollas, G. H. *Trans. Faraday Soc.* 1960, *56*, 1165. [c] Topp, N. E.; Davies, C. W. *J. Chem. Soc.* 1940, 87. [d] Cannon, R. K.; Kibrick, A. *J. Am. Chem. Soc.* 1938, *60*, 2314. [e] Kahmann, K.; Martell, A. E. *Inorg. Chem.* 1965, *4*, 462. [f] Reference 3; mal = maleate. [g] McNevin, W. M.; Kriedge, O. H. *J. Am. Chem. Soc.* 1955, *77*, 6149. [h] Reference 18. [i] Datta, S. P.; Brzybowski, A. K.; Weston, B. A. *J. Chem. Soc.* 1958, *80*, 4180.

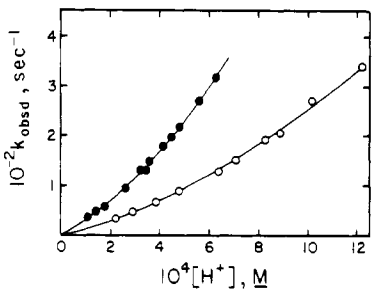

Figure 3. Dependence of k_{obsd} on the concentration of H_3O^+ (pH <4) in the presence of (○) 0.010 M and (●) 0.10 M chloroacetic acid. The calculated curves were determined by using eq 12 and the resolved constants given in Table IV.

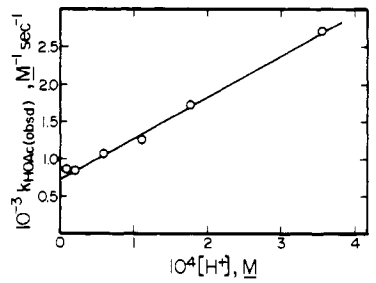

Figure 4. Dependence of k_{HOAc}(obsd) on the concentration of H_3O^+, where k_{HOAc}(obsd) is given by $k_{HOAc} + k_{H,HOAc}[H^+]$ (eq 12).

rapid protonation of $Ni(H_{-2}G_3)^-$ occurs prior to the rate-limiting reaction with HB. With the assumption of negligible concentrations of $Ni(H_{-2}G_3)H$, the first-order rate constant will be given by eq 12, where $k_{H,H} = k^H{}_H K_H$ and $k_{H,HB} = k^H{}_{HB} K_H$. The solid curves in Figure 3 were calculated by using eq 12 and the resolved rate constants given in Table IV. In each case, the fraction of total acid concentration present as HB was determined from the ratio $[H^+]/([H^+] + K_a)$. Similar H_3O^+ dependences are observed in the presence of glycolic and formic acids (Table III) where the resolved rate constants are reported in Table IV. General-acid catalysis was studied extensively for acetic acid (Table V) between pH 3.5 and 5.2. At each pH value, a linear dependence between k_{obsd} and $[HOAc]_T$ was observed. Resolution of the acetic acid rate constants (k_{HB}, $k_{H,HB}$) is shown in Figure 4, where k_{HOAc}(obsd)

$$k_{obsd} = k_{H_2O} + (k_H + k_{H,H}[H^+])[H^+] + (k_{HB} + k_{H,HB}[H^+])[HB] \quad (12)$$

Table III. Observed Rate Constants for the Reaction of $Ni(H_{-2}G_3)^-$ with H_3O^+ in the Presence of HB (0.30 M $NaClO_4$, 25.0 °C)[a]

−log [H⁺]	k_{obsd}, s^{-1}	−log [H⁺]	k_{obsd}, s^{-1}
	0.15 M $[MES]_T$		
6.23	0.142 ± 0.001	5.72	0.271 ± 0.001
6.15	0.151 ± 0.001	5.62	0.311 ± 0.001
5.93	0.199 ± 0.001	5.53	0.366 ± 0.002
	0.10 M $[ClCH_2CO_2H]_T$		
3.95	34 ± 3	3.45	150 ± 5
3.85	44.6 ± 0.1	3.38	185 ± 3
3.75	56 ± 4	3.35	198 ± 3
3.58	96.5 ± 0.6	3.32	222 ± 4
3.47	135 ± 2	3.25	270 ± 8
3.46	137 ± 1	3.21	322 ± 4
	0.01 M $[ClCH_2CO_2H]_T$		
3.65	31.9 ± 0.5	3.15	148 ± 2
3.53	46.3 ± 0.6	3.08	195 ± 4
3.41	63.0 ± 0.8	3.05	205 ± 9
3.32	90 ± 1	2.99	270 ± 10
3.19	130 ± 2	2.91	340 ± 20
	0.15 M Glycolic Acid		
4.23	60.2 ± 0.5	3.83	147 ± 3
4.02	96 ± 1	3.64	225 ± 4
3.92	119 ± 1		
	0.15 M Formic Acid		
4.23	38.0 ± 0.3	3.82	101 ± 2
4.10	52.3 ± 0.6	3.70	142 ± 3
3.97	70.7 ± 0.8	3.59	186 ± 3
3.84	97.1 ± 0.3		

[a] $[Ni(H_{-2}G_3)^-]_T = 1.0 \times 10^{-3}$ M, 430 nm.

Table IV. General-Acid Rate Constants for the Reaction of HB with $Ni(H_{-2}G_3)^-$ (k_{HB}) and $Ni(H_{-2}G_3)H$ ($k_{H,HB}$) (0.30 M $NaClO_4$, 25.0 ± 0.1 °C)

HB	pK_a(HB)	k_{HB}, M^{-1} s^{-1}	$k_{H,HB}$, M^{-2} s^{-1}
H_3O^+	−1.74	9.5×10^4 (k_H)	1.1×10^8 ($k_{H,H}$)
chloroacetic	2.86[a]	1.9×10^3	8.4×10^6
formic	3.75[b]	5.8×10^2	4.5×10^6
glycolic	3.83[c]	9.4×10^2	5.3×10^6
acetic	4.64[d]	7.7×10^2	5.5×10^6

[a] Wright, D. D. *J. Am. Chem. Soc.* 1934, *56*, 314. [b] Harned, H. S.; Embree, N. D. *Ibid.* 1934, *56*, 1042. [c] Nims, L. F. *Ibid.* 1936, *58*, 987. [d] Feldman, I.; Kovel, L. *Inorg. Chem.* 1963, *2*, 145.

Table V. Observed Rate Constants for the Reaction of $Ni(H_{-2}G_3)^-$ with Acetic Acid (0.30 M $NaClO_4$, 25.0 °C)[a]

$[HOAc]_T$, M[b]	−log [H⁺]	k_{obsd}, s^{-1}	$[HOAc]_T$, M[b]	−log [H⁺]	k_{obsd}, s^{-1}
0.020	3.77	86 ± 2	0.080	5.18	15.5 ± 0.1
0.020	3.46	197 ± 2	0.10	4.67	42.8 ± 0.3
0.040	3.74	120 ± 2	0.10	3.97	136 ± 2
0.040	3.44	266 ± 3	0.14	4.20	112 ± 1
0.060	5.18	11.9 ± 0.1	0.14	3.95	179 ± 1
0.060	4.70	26.1 ± 0.3	0.20	5.12	41.7 ± 0.2
0.060	4.27	50.9 ± 0.5	0.20	4.64	84.6 ± 0.9
0.060	3.74	148 ± 1	0.20	4.16	161 ± 1
0.060	3.45	299 ± 4	0.20	3.94	236 ± 2

[a] $[Ni(H_{-2}G_3)^-]_T = 1.0 \times 10^{-3}$ M, 430 nm. [b] −log [H⁺] > 4.0, 0.10 M $[MES]_T$; −log [H⁺] < 4.0, 0.10 M $[ClCH_2CO_2H]_T$.

$= k_{HOAc} + k_{H,HB}[H^+]$ from eq 12.

The H,HB pathway proposed for the $Ni(H_{-2}G_3)^-$ acid decomposition reaction involves a rapid peptide oxygen (or carboxylate) protonation (Scheme II) prior to the rate-limiting reaction with HB. A similar pathway has been proposed for the protonation reactions of $Ni(H_{-3}G_4)^{2-}$ (tetraglycine), $Ni(H_{-3}G_3a)^-$ (triglycinamide), and $Ni(H_{-3}G_4a)^-$ (tetraglycinamide), where an outside-protonated complex is formed prior to bond rupture.[4,14] However, unlike the outside-protonated complexes of $Ni(H_{-3}G_3a)^-$ and $Ni(H_{-3}G_4)^{2-}$, $Ni(H_{-2}G_3)H$ is subject to general-acid catalysis by HB. Equations 10 and 11 propose that the addition of an outside proton (with a stability constant K_H) is followed by HB attack with the rate constant k_{HB}^H. At −log [H⁺] ≥ 2.9 the concentration of the $Ni(H_{-2}G_3)H$ species is negligible and, therefore, only the product $k^H_{HB}K_H$ ($=k_{H,HB}$) could be evaluated. Below −log [H⁺] values of 2.9, the reactions become too rapid (k_{obsd} > 400 s^{-1}) to measure by stopped-flow techniques. Because of these limitations, only an upper limit of $K_H \leq 10^{2.2}$ M^{-1} can be estimated for the outside-protonation constant of $Ni(H_{-2}G_3)^-$.

Scheme II. Outside-Protonation Reaction

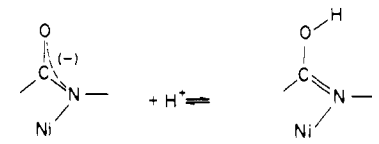

A comparison between the general-acid rate constants (Table IV) for $Ni(H_{-2}G_3)^-$ and $Ni(H_{-2}G_3)H$, where $K_H \leq 10^{2.2}$ M^{-1}, shows that (1) the outside protonation increased the effectiveness of acid catalysis by at least a factor of 10 and (2) both k^H_{HB} and k_{HB} exhibit the same type of dependence on the acidity of HB, namely, that both rate constants increase as the acidity of HB increases. Although $Ni(H_{-2}G_3)^-$ is a square-planar, diamagnetic complex, the structure of $Ni(H_{-2}G_3)H$ is less certain because appreciable concentrations of the outside-protonated complex were not kinetically or spectrophotometrically (430 nm) detected. However, the mono-outside-protonated nickel(II) complexes of tetraglycine and tetraglycinamide $Ni(H_{-3}G_4)H^-$ and $Ni(H_{-3}G_4a)H$ can be transiently formed in appreciable concentrations, and their visible spectra are consistent with those of other square-planar nickel(II)–peptide complexes.[4,14] Hence, it is reasonable to assume that the $Ni(H_{-2}G_3)H$ species will also be square-planar and diamagnetic.

The two peptide oxygens and the coordinated carboxylate group of $Ni(H_{-2}G_3)^-$ (structure I) provide three potential sites for outside protonation. For each site, the availability of the oxygen electron pairs will permit a rapid proton transfer equivalent to normal acid–base reactions followed by the rate-limiting reaction of HB with the peptide nitrogen. The nature of the protonation sites gives some insight into the details of the acid-catalyzed decomposition of $Ni(H_{-2}G_3)H$. The ability of the peptide nitrogen to accept a proton will depend on which oxygen site has been protonated in $Ni(H_{-2}G_3)$ species. Peptide oxygen protonation will give a coordinated imine group (Ni—N=C—OH), which lacks the readily available electron pair required for subsequent acid attack. This suggests that the peptide nitrogen and oxygen protonations are occurring at two different peptide residues. The increased reactivity of $Ni(H_{-2}G_3)H$ to acid catalysis may be due to the ability of the outside proton to decrease the crystal field strength of the nickel(II) square-planar complex. As a result, it becomes easier to transfer a proton to the peptide nitrogen and break the nickel–peptide bond.

$[Ni(H_{-2}G_3)(\alpha\text{-pic})]^-$ and $[Ni(H_{-2}G_3)Im]^-$ Complexes. Both α-picoline and imidazole form ternary complexes with $Ni(H_{-2}G_3)^-$. The absorbance at 430 nm as a function of both imidazole and α-picoline concentrations is given in Figure 5. The calculated curves were determined by using eq 2 with the resolved molar absorptivities and formation constants given in Table VI.

(14) Raycheba, J. M. T.; Margerum, D. W. *Inorg. Chem.* **1980**, *19*, 497.

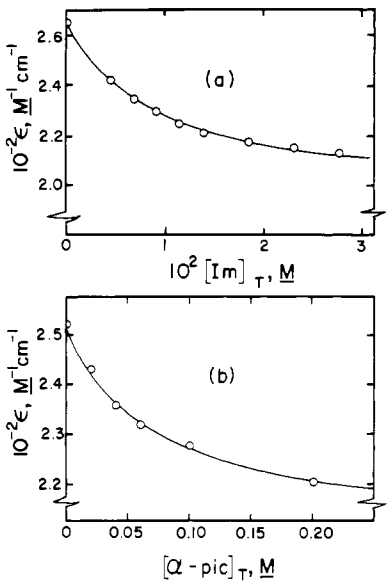

Figure 5. Dependence of the molar absorptivity (430 nm) of $[Ni(H_{-2}G_3)^-]_T$ on the concentration of (a) imidazole and (b) α-picoline. The solid curves were calculated by using eq 2 and the constants given in Table VII.

Table VI. Spectrophotometrically Determined Equilibrium Constants for $[Ni(H_{-2}G_3)B]^-$ (0.30 M $NaClO_4$, 25.0 ± 0.1 °C)

complex	K_B, M^{-1} [a]	ϵ_{NiLB}, M^{-1} cm^{-1} [b]
$[Ni(H_{-2}G_3)Im]^-$	106	209
$[Ni(H_{-2}G_3)(\alpha\text{-pic})]^-$	13.9	194
$[Ni(H_{-2}G_3)(2,6\text{-lut})]^-$ [c]	11 [d]	

[a] For the equilibrium

$$Ni(H_{-2}G_3)^- + B \overset{K}{\rightleftharpoons} [Ni(H_{-2}G_3)B]^-$$

[b] ϵ_{NiL} = 260 M^{-1} cm^{-1}, 430 nm. [c] 2,6-lut = lutidine. [d] 0.10 M $NaClO_4$; see ref 16.

The molar absorptivities (430 nm) for $[Ni(H_{-2}G_3)(\alpha\text{-pic})]^-$ (194 M^{-1} cm^{-1}) and $[Ni(H_{-2}G_3)Im]^-$ (209 M^{-1} cm^{-1}) compared with that of $Ni(H_{-2}G_3)^-$ (260 M^{-1} cm^{-1}) suggest that these ternary complexes have square-planar geometries.[4,15] The proposed structure of the α-picoline complex (structure II) is one in which the α-picoline has displaced the coordinated

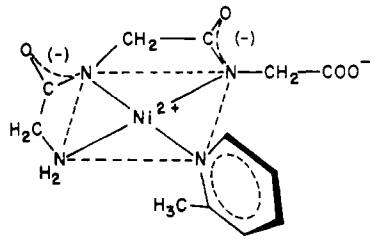

II

carboxylate group of $Ni(H_{-2}G_3)^-$, and the methyl substituent sterically blocks one axial coordination site of the nickel(II). A similar structure has been proposed for the 2,6-lutidine complex of $Ni(H_{-2}G_3)^-$.[16]

Imidazole and α-Picoline Acid Catalysis. The reactions of $Ni(H_{-2}G_3)^-$ with the general acids α-picoline and imidazole were studied as a function of pH and acid concentration (Table VII). For both acids, initial absorbance jumps, corresponding to the rapid formation of the ternary complex, were observed prior to acid decomposition.

Table VII. Observed Rate Constants for the Reaction of $Ni(H_{-2}G_3)^-$ with α-Picoline and Imidazole (0.30 M $NaClO_4$, 25.0 °C)[a]

$[HB]_T$, M	−log $[H^+]$	k_{obsd}, s^{-1}	$[HB]_T$, M	−log $[H^+]$	k_{obsd}, s^{-1}
		HB = α-Picoline[b]			
0.050	6.13	0.261 ± 0.001	0.18	5.98	0.485 ± 0.002
0.050	5.94	0.338 ± 0.001	0.20	6.22	0.356 ± 0.001
0.10	6.18	0.316 ± 0.001	0.20	6.19	0.369 ± 0.001
0.10	6.16	0.322 ± 0.002	0.20	6.02	0.475 ± 0.002
0.10	6.00	0.401 ± 0.001	0.25	6.23	0.359 ± 0.001
0.10	5.96	0.415 ± 0.001	0.25	6.07	0.471 ± 0.001
		HB = α-Picoline, 0.050 M $[HOAc]_T$			
0	6.14	1.48 ± 0.01	0.125	6.16	1.13 ± 0.01
0.025	6.14	1.39 ± 0.02	0.175	6.17	1.06 ± 0.01
0.050	6.14	1.31 ± 0.01	0.20	6.17	1.02 ± 0.02
0.075	6.15	1.25 ± 0.01			
		HB = Imidazole[b]			
0	6.12	0.143 ± 0.001	0.0805	6.43	1.50 ± 0.01
0.0230	6.11	0.411 ± 0.002	0.104	6.43	1.98 ± 0.02
0.0460	6.12	0.783 ± 0.001	0.150	6.43	3.01 ± 0.03
0.115	6.12	1.93 ± 0.02	0.196	6.44	3.98 ± 0.02
0.161	6.12	2.80 ± 0.02	0	6.61	0.103 ± 0.001
0	6.44	0.144 ± 0.001	0.0230	6.62	0.417 ± 0.002
0.0115	6.43	0.270 ± 0.001	0.0920	6.60	1.74 ± 0.02
0.0230	6.41	0.440 ± 0.001	0.138	6.61	2.81 ± 0.02
0.0460	6.43	0.835 ± 0.001	0.161	6.60	3.42 ± 0.03

[a] $[Ni(H_{-2}G_3)^-]_T = 1.0 \times 10^{-3}$ M, 430 nm. [b] 0.10 M $[MES]_T$.

Table VIII. General-Acid Rate Constants for the Protonation of $Ni(H_{-2}G_3)^-$ and $[Ni(H_{-2}G_3)B]^-$ (0.30 M $NaClO_4$, 25.0 °C)

complex	HB	k_{HB}, M^{-1} s^{-1}	k_B, M^{-1} s^{-1}
$Ni(H_{-2}G_3)^-$	$H(Im)^+$ [a]	1.4	
	$H(\alpha\text{-pic})^+$ [b]	6.3	
$[Ni(H_{-2}G_3)Im]^-$	$H(Im)^+$	1.7	46
$[Ni(H_{-2}G_3)(\alpha\text{-pic})]^-$	$H(\alpha\text{-pic})^+$	<0.2	

[a] pK_a = 7.2: Brooks, P.; Davidson, N. *J. Am. Chem. Soc.* **1960**, *82*, 2118. [b] pK_a = 6.06: Kahmann, K.; Siegel, H.; Erlenmeyer, H. *Helv. Chim. Acta* **1964**, *47*, 1754.

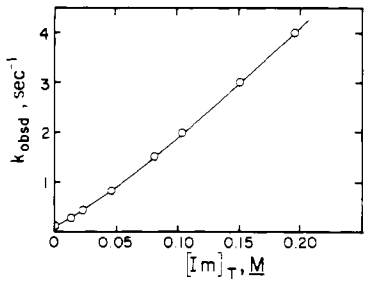

Figure 6. Dependence of k_{obsd} on the concentration of imidazole. The calculated curve was determined by using eq 16 and the resolved constants given in Tables VII and VIII.

In the pH range studied, the kinetic behavior observed for the reaction of imidazole, B, with $Ni(H_{-2}G_3)^-$ (Figure 6) can be described by eq 6 and 7 and eq 13–15. The rapid formation

$$Ni(H_{-2}G_3)^- + B \overset{K_B}{\rightleftharpoons} [Ni(H_{-2}G_3)B]^- \quad (13)$$

$$[Ni(H_{-2}G_3)B]^- + HB \xrightarrow{k^B_{HB}} [Ni(H_{-1}G_3)B] + B \quad (14)$$

$$[Ni(H_{-1}G_3)B] + 2H^+ \xrightarrow{fast} Ni^{2+}(aq) + HG_3^{\pm} + B \quad (15)$$

and the subsequent acid decomposition of the ternary complex $[Ni(H_{-2}G_3)B]^-$ are accounted for by eq 13–15. The first-order

(15) Barefield, E. K. Ph.D. Thesis, The Ohio State University, Columbus, Ohio, 1969.
(16) Raycheba, J. M. T.; Margerum, D. W. *Inorg. Chem.* **1980**, *19*, 837.

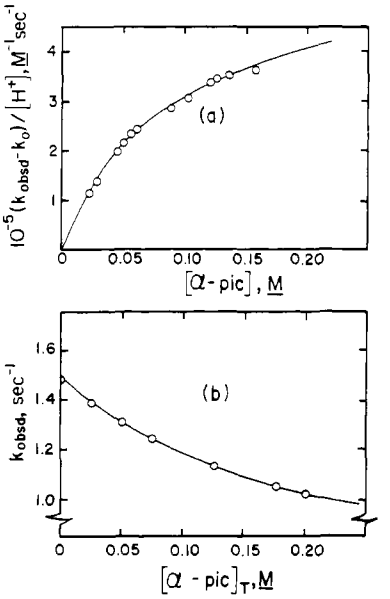

Figure 7. (a) Dependence of the pH-corrected first-order rate constant (eq 17) on the concentration of α-picoline. (b) Dependence of k_{obsd} on the concentration of α-picoline (−log $[H^+]$ = 6.16) in the presence of 0.050 M acetic acid. The calculated curves were determined by using eq 18, the constants given in Tables VII and VIII, and k_{HOAc} = 7.7 × 10^2 M s^{-1}.

rate constant for protonation of both $Ni(H_{-2}G_3)^-$ and $[Ni(H_{-2}G_3)Im]^-$ is given by eq 16, where k_0 equals $k_{H_2O} + k_H[H^+]$

$$k_{obsd} = \frac{k_0 + k_{HB}[HB] + k^B_{HB}K_B[B][HB]}{1 + K_B[B]} \quad (16)$$

and k_{HB} is defined by eq 5. The calculated curve in Figure 6 was determined by using eq 16 and the resolved rate constant and formation constants given in Tables VIII and VI, respectively.

For $[Ni(H_{-2}G_3)Im]^-$, a pathway (Table VIII), in which the ternary complex is subject to a nucleophilic attack (k_B^B) by imidazole, is observed. This pathway is similar to the nucleophilic reactions observed for $Ni(H_{-2}G_3)^-$ (eq 8 and 9).[13] Imidazole is a more effective nucleophile with $[Ni(H_{-2}G_3)Im]^-$ (k_{Im}^{Im} = 46 M^{-1} s^{-1}) compared with $Ni(H_{-2}G_3)^-$ (k_{Im} < 2 M^{-1} s^{-1}) because the triglycine ligand is partially displaced in $[Ni(H_{-2}G_3)Im]^-$. With $Ni(H_{-2}G_3)^-$, both the bound carboxylate and one peptide nitrogen group must be displaced before or during the rate-determining step.

The primary kinetic difference between the ternary complexes with α-picoline and imidazole is the dissociation of the $[Ni(H_{-2}G_3)(\alpha\text{-pic})]^-$ complex is not general-acid catalyzed. This is illustrated by the α-picoline inhibition of the acetic acid catalysis of the $Ni(H_{-2}G_3)^-$ dissociation (Figure 7). With k^B_{HB} = 0 for α-picoline (B), eq 16 simplifies to eq 17. In the

$$k_{obsd} = \frac{k_0 + k_{HB}[HB]}{1 + K_B[B]} \quad (17)$$

presence of acetic acid, general-acid catalysis of the $Ni(H_{-2}G_3)^-$ dissociation by both $H(\alpha\text{-pic})^+$ (k_{HB}) and HOAc (k_{HOAc}) occurs. Under these conditions, the first-order rate constant is described by eq 18. The calculated curves in

$$k_{obsd} = \frac{k_0 + k_{HOAc}[HOAc] + k_{HB}[HB]}{1 + K_B[B]} \quad (18)$$

Figure 7 were evaluated with use of eq 17 and 18, the spectrophotometrically determined formation constant (Table VI), and the resolved rate constants given in Table VIII.

Brønsted Plot. A plot of log k_{HB} against the pK_a values for HB is given in Figure 1. The results confirm a gradual change in the Brønsted slope (α value) for acids with pK_a values less than 5 and indicate that the value for H_3O^+ is not anomalous but is consistent with the trend for other strong acids. Significant deviations from the Brønsted curve occur for the acids H_2O and $H(ox)^-$ (ox = oxalate), which are more effective at peptide protonation than calculated. Recent deuterium studies have shown that water acts as a Brønsted acid in its reaction with $Ni(H_{-2}G_3)^-$.[17] Other acids that have been reported to show similar behavior for $Ni(H_{-2}G_3)^-$ protonation are $H_2PO_4^-$ and HCO_3^-.[3,4] All four acids (H_2O, $H(ox)^-$, $H_2PO_4^-$, and HCO_3^-) have the ability to act as Lewis bases as well as Brønsted acids. With such coordinating acids, the peptide protonation by the Brønsted acid is assisted by the simultaneous coordination of the basic portion of the general acid to the nickel(II) center.

The importance of steric hindrance in $Ni(H_{-2}G_3)^-$ proton-transfer reactions is illustrated by the lack of general-acid catalysis of both $H(MES)^\pm$ and $H(PIPES)^-$.[18] The reduced catalytic effectiveness of $H(MES)^\pm$ and $H(PIPES)^-$ makes these two acids excellent buffers for studying general-acid catalysis of $Ni(H_{-2}G_3)^-$, because even at moderately high concentrations the buffer makes only a minimal contribution to the observed proton-transfer rate.

The curve (solid line) for the Brønsted plot in Figure 1 can be described by a modified[8,9] Marcus theory[10,11] (eq 19–21)

$$\Delta G^\ddagger = W_R + \frac{\lambda}{4}\left(1 + \frac{\Delta G_{HB} - C}{\lambda}\right)^2 \quad (19)$$

$$|\Delta G^\circ_{HB} - C| \le \lambda$$

$$\Delta G^\ddagger = W_R \qquad (\Delta G^\circ_{HB} - C) < -\lambda \quad (20)$$

$$\Delta G^\ddagger = \Delta G^\circ_{HB} + W_R - C \qquad (\Delta G^\circ_{HB} - C) > \lambda \quad (21)$$

where $C = \Delta G^\circ_{Ni(H_{-1}L)} - W_P + W_R$. W_R (or W_P) is the work required to bring the reactants (or products) together, including that necessary for solvent reorientation, to form the reaction complex. The work term accounts for that part of the total energy barrier ($\Delta G^\ddagger$) that is independent of the free energy change of the reaction ($\Delta G^\circ = \Delta G^\circ_{HB} - \Delta G^\circ_{Ni(H_{-1}L)}$). Within the reaction complex, the energy barrier for proton transfer is determined by the magnitude of the intrinsic energy barrier ($\lambda/4$) and the free energy change of the reaction (ΔG°). The calculated Brønsted curve was determined with use of eq 19–21, where $k_{HB} = (\bar{k}T/h)\exp(-\Delta G^\ddagger/RT)$.[11] The results of the nonlinear analysis (excluding the acids H_2O, $H(ox)^-$, $H(MES)^\pm$, and $H(PIPES)^-$) are W_R = 10.5 kcal mol^{-1}, $\lambda/4$ = 1.6 kcal mol^{-1}, and C = 3.5 kcal mol^{-1}. The Marcus parameters indicate that the free energy of activation for peptide protonation is dominated by the work (W_R) required to form the reaction complex.

Peptide protonation of $Ni(H_{-2}G_3)^-$ to give $Ni(H_{-1}G_3)$ is accompanied by both a change in nickel(II) geometry from square planar to octahedral and metal–nitrogen bond rupture. The importance of metal ion solvation for $Ni(H_{-2}G_3)^-$ protonation is illustrated by the lack of general-acid catalysis (Table VIII) for protonation of the ternary complex $[Ni(H_{-2}G_3)(\alpha\text{-pic})]^-$, where the methyl substituent of the coordinated α-picoline (structure II) prevents square-planar to octahedral conversion. On the other hand, general-acid catalysis is readily observed for $[Ni(H_{-2}G_3)Im]^-$, where no hindrance to axial coordination by water exists. Blocking of metal ion solvation may increase W_R or $\lambda/4$ or both and thus

(17) Bannister, C. E.; Youngblood, M. P.; Young, D. C.; Margerum, D. W., to be submitted for publication.

(18) MES = 2-(*N*-morpholino)ethanesulfonic acid; PIPES = piperazine-*N*,*N*'-bis(2-ethanesulfonic acid). Good, N. E.; Winget, G. D.; Winter, W.; Connolly, T. N.; Izawa, S.; Singh, R. M. M. *Biochemistry* **1966**, *5*, 467.

inhibits the general-acid-catalyzed dissociation pathway. Within the reaction complex, the increased electron density on the peptide nitrogen caused by solvent-assisted bond weakening permits unhindered proton transfer to occur. This is reflected by the low value obtained for the intrinsic energy barrier $\lambda/4$.

The product work term (W_P) is 17.4 kcal mol^{-1} and is calculated from C and the acid-dissociation constant ($10^{-7.7}$ M) of Ni($H_{-1}G_3$).[3] Formation of the reaction complex from the products (Ni($H_{-1}G_3$), B) would require bringing the products together with coordination of the peptide linkage. The large value of W_P is a reflection of the poor coordinating ability of the protonated peptide nitrogen.

Acknowledgment. This investigation was supported by the National Science Foundation (Grant CHE74-00043) and the Public Health Service (Grant No. GM 12152 from the National Institute of General Medical Sciences).

Registry No. Ni($H_{-2}G_3$)$^-$, 31011-65-1; [Ni($H_{-2}G_3$)Im]$^-$, 78393-22-3; [Ni($H_{-2}G_3$)(α-pic)]$^-$, 78393-23-4.

Contribution from the Department of Chemistry, State University of New York at Stony Brook, Stony Brook, New York 11794

Formation of Nitrosyltricyanonickelate ($NiNO(CN)_3^{2-}$) in a Direct NO^- Displacement Reaction[1]

FRANCIS T. BONNER* and MOHAMMAD JAVAID AKHTAR

Received April 6, 1981

Kinetic and stoichiometric studies of the formation of the violet complex $NiNO(CN)_3^{2-}$ when trioxodinitrate ($Na_2N_2O_3$) decomposes in the presence of $Ni(CN)_4^{2-}$ show that the process is controlled by release of the intermediate species HNO from $HN_2O_3^-$. Nitrosyltricyanonickelate is formed by direct displacement of CN^- by NO^-, in competition with dimerization of the intermediate to form N_2O. The proportion of NO^- that is trapped by $Ni(CN)_4^{2-}$ is pH dependent, increasing from 3.6% at pH 9.27 to ca. 30% at pH 10.75 with $Ni(CN)_4^{2-}$ in twofold excess over $Na_2N_2O_3$. In the additional presence of NH_2OH (tenfold excess), a three-way competiton for NO^- is established in which reduction to N_2 predominates and in which trapping of NO^- by $Ni(CN)_4^{2-}$ is reduced to 1.27% at pH 10.82. A NO^- intermediate known to be produced in the reaction between NO and NH_2OH is also shown to form $NiNO(CN)_3^{2-}$ by a direct displacement interaction with $Ni(CN)_4^{2-}$. The trapping efficiency of $Ni(CN)_4^{2-}$ for NO^- from this source is less than that for NO^- from $HN_2O_3^-$ decomposition. This difference is ascribed to a probable difference in the electronic states of NO^- ions formed in the two cases.

Introduction

In 1948 Nast and Proeschel[2,3] demonstrated that the deep violet product of the reaction between $K_2Ni(CN)_3$ and NO in liquid ammonia is identical with the complex ion produced by the action of hydroxylamine on $K_2Ni(CN)_4$ in alkaline aqueous solution. The product complex is $NiNO(CN)_3^{2-}$ and was postulated to have a tetrahedral rather than square-planar configuration.[2] Nast et al.[3] proposed that the disproportionation of hydroxylamine produces HNO, which is then deprotonated, and that NO^- directly displaces CN^- in $Ni(CN)_4^{2-}$ (eq 1–3). Nast, Nyul, and Grziwok[4] proposed that the yellow

$$2NH_2OH = NH_3 + HNO + H_2O \quad (1)$$

$$HNO + OH^- = NO^- + H_2O \quad (2)$$

$$Ni(CN)_4^{2-} + NO^- = NiNO(CN)_3^{2-} + CN^- \quad (3)$$

to violet color change accompanying postulated reaction 3 could be used as a sensitive test for the intermediacy of HNO or NO^-. They applied it, with apparently positive results, to the alkaline hydrolyses of three hydroxylamine sulfonates. Kinetic evidence for the intermediacy of HNO (or NOH) in one of these cases, the hydrolysis of hydroxylamine *N*-sulfonate, was later reported by Ackerman and Powell.[5]

The decomposition of trioxodinitrate ($Na_2N_2O_3$) has been assumed to yield HNO (or NOH) since the time of its discovery by Angeli,[6] an assumption that has been verified by isotope labeling.[7] If displacement reaction 3 occurs, $Na_2N_2O_3$ decomposition in the presence of $K_2Ni(CN)_4$ should produce the characteristic violet color of $NiNO(CN)_3^{2-}$. Veprek-Siska et al. observed such a reaction (eq 4) and employed it in

$$N_2O_3^{2-} + Ni(CN)_4^{2-} = NiNO(CN)_3^{2-} + NO_2^- + CN^- \quad (4)$$

development of a colorimetric analytical method for trioxodinitrate.[8] Otherwise, Nast's proposed test for HNO appears to have recieved little attention, although Hughes and Nicklin[9] applied it in a study of the autoxidation of hydroxylamine.

Veprek-Siska and Lunak have reported kinetic studies of the NH_2OH–$Ni(CN)_4^{2-}$ reaction in the presence of O_2[10] and in an inert atmosphere.[11] They conclude that displacement of CN^- by NO^- does not occur in either case, that trapping of NO^- cannot account for the observations of Hughes and Nicklin,[9] and that Nast's proposed test[4] for NO^- is not valid. In the oxidative case they postulate coordination of a fully deprotonated hydroxylamino species NO^{3-}, followed by its

(1) Research supported by the National Science Foundation, Grant No. 78-24176.
(2) Nast, R.; Proeschel, E. *Z. Anorg. Chem.* **1948**, *256*, 145.
(3) Nast, R.; Proeschel, E. *Z. Anorg. Chem.* **1948**, *256*, 159.
(4) Nast, R.; Nyul, K.; Grziwok, E. *Z. Anorg. Allgem. Chem.* **1952**, *267*, 305.
(5) Ackermann, M. N.; Powell, R. E. *Inorg. Chem.* **1966**, *8*, 1334.
(6) Angeli, A. *Gazz. Chim. Ital.* **1903**, *33*, 245.
(7) Bonner, F. T.; Ravid, B. *Inorg. Chem.* **1975**, *14*, 558.
(8) Veprek-Siska, J.; Smirous, F.; Pliska, V. *Collect. Czech. Chem. Commun.* **1959** *24*, 1175.
(9) Hughes, M. N.; Nicklin, H. G. *J. Chem. Soc. A* **1971**, 164.
(10) Veprek-Siska, J.; Lunak, S. *Collect. Czech. Chem. Commun.* **1972**, *37*, 3846.
(11) Veprek-Siska, J.; Lunak, S. *Collect. Czech. Chem. Commun.* **1974**, *39*, 41.

0020-1669/81/1320-3155$01.25/0